# Harmonic inpainting of the cosmic microwave background sky: Formulation and error estimate

Kaiki Taro Inoue
*Department of Science and Engineering, Kinki University, Higashi-Osaka, Japan*

Paolo Cabella
*Universitá La Sapienza, Universitá Tor Vergata, Rome, Italy*

Eiichiro Komatsu
*Department of Astronomy, The University of Texas at Austin, Texas, USA*
(Received 3 April 2008; published 27 June 2008)

We develop a new interpolation scheme, based on harmonic inpainting, for reconstructing the cosmic microwave backgroundtemperature data within the Galaxy mask from the data outside the mask. We find that, for scale-invariant isotropic random Gaussian fluctuations, the developed algorithm reduces the errors in the reconstructed map for the odd-parity modes significantly for azimuthally symmetric masks with constant galactic latitudes. For a more realistic Galaxy mask, we find a modest improvement in the even-parity modes as well.

DOI: 10.1103/PhysRevD.77.123539 PACS numbers: 98.80.−k, 04.25.Nx, 98.70.Vc

## I. INTRODUCTION

After the first release of the cosmic microwave background (CMB) anisotropy data from the Wilkinson Microwave Anisotropy Probe (WMAP) in 2003, various types of ''anomalies'' in the CMB temperature anisotropy on large angular scales have been reported [1–10]. The origin of these anomalies—whether they are cosmological, statistical fluke, or something else—is unknown [11–18].

Recent analyses based on either a Bayesian or frequentist approach show that the statistical significance level of some of the large-angle anomalies is sensitive to the treatment of the galactic sky cut [19,20]. The lack of robustness mainly comes from the fact that we cannot use the full-sky information, but can only use a part of the sky outside the Galaxy mask. There is a way to construct a full-sky map that minimizes the foreground contamination, e.g., the internal linear combination (ILC) technique [21,22]; however, we cannot rule out a potential residual foreground contamination in the ILC map, especially in the region that is very close to the galactic plane, due to a limited number of sky maps at different frequencies.

An alternative approach is to *reconstruct* the temperature data within the Galaxy mask from the information available outside the mask. So far, various types of methods, such as the direct inversion, the Wiener filtering, and the power equalization filtering, have been proposed for reconstructing the CMB anisotropy on the cut sky [23]. The Gibbs sampling [24] provides a way to compute an ensemble of the Wiener filtered maps with a statistical sample of power spectra fit to a given input sky map, which can be used to estimate the best-fitting Wiener filtered map and the corresponding uncertainties; see [25] and references therein. All these methods are based upon a linear transformation of the expansion coefficients of spherical harmonics on the cut sky, $a_{lm}^{\rm cut}$, into the full-sky coefficients $a_{lm}^{\rm full}$, which are suitable for nearly all-sky data with a small sky cut. However, it has been shown that the methods do not work properly for maps with a large sky cut [26,27].

In order to reconstruct the data within the Galaxy mask, one needs to assume a prior on the properties of the data. For instance, one may require the temperature anisotropies and their absolute values of the gradient to have a Gaussian distribution. Then, one can find an optimal solution for reconstructing the data within the masked region from available information outside the mask. Such an operation is called an ''inpainting,'' which has been used by skilled museum or art workers for restoring damaged photographs, films, and paintings. In recent years, various automatic inpainting algorithms based on partial differential equations or the variational principle have been proposed and used for automatic image restoration and removal of occlusions [28–30].

In this paper, we formulate an algorithm based on harmonic inpainting for reconstructing smooth CMB data within the Galaxy mask. In Sec. II, we develop a numerical scheme for implementing harmonic inpainting on a unit sphere based on the boundary element method. In Sec. III, we use Monte Carlo simulations to estimate the errors of the inpainted signal for azimuthally symmetric sky cuts as well as for a realistic nonsymmetric cut. In Sec. IV, we summarize our results.

## II. HARMONIC INPAINTING

Let $\mathbf{x} = \mathbf{x}(\theta, \phi)$ be a unit pointing vector on the sky toward a given direction $(\theta, \phi)$ and $u_0(\mathbf{x})$ be an observed temperature fluctuation outside the Galaxy mask $\mathbf{x} \in \bar{D}$, where $D$ denotes the region within the mask (an open connected set) and $\bar{D}$ outside the mask (the complement

 

of $D$). We assume that the boundary of $D$, $\partial D$ is smooth. We wish to reconstruct a smooth temperature fluctuation on the full-sky, or a best inpainting $u(\mathbf{x})$ from the data outside the mask $u_0(\mathbf{x})$.

We reconstruct the full-sky map $u(\mathbf{x})$ by locally minimizing the following "energy":

$$\mathcal{H}[u] = \int_{S^2} [\lambda(u - u_0)^2 + |\nabla u|^2]\sqrt{g}dv_{\mathbf{x}}, \tag{2.1}$$

where $\lambda$ is a positive constant, $g_{ij}$ is the Riemannian metric tensor of a sphere, and $dv$ is the infinitesimal Euclidean volume. The first term and the second term in the right-hand side of Eq. (2.1) represent faithfulness to the imperfect data and the regularization penalty, respectively. The constant $\lambda$ controls a tradeoff between faithfulness to the imperfect data and smoothness of the fluctuations. This procedure is optimal when the absolute values of the gradient $|\nabla u|$ and the difference between $u$ and $u_0$ are Gaussian distributed.[1] The Euler-Lagrange equation of (2.1) is given by

$$-\Delta u + \lambda(u - u_0) = 0; \qquad \begin{matrix} \lambda > 0 & \text{for } \mathbf{x} \notin D, \\ \lambda = 0 & \text{for } \mathbf{x} \in D. \end{matrix} \tag{2.2}$$

In order to solve Eq. (2.2), we also need a solution for the derivative of $u$ with respect to the unit vector $n$ normal to the boundary of the mask

$$q \equiv \frac{\partial u}{\partial n} = \left(\frac{\partial u}{\partial x^i}\right) n^i, \tag{2.3}$$

where $\mathbf{x} \in \partial D$ for which $u$ and $q$ are continuous.

The minimizer of Eq. (2.1) is called the harmonic inpainting denoizing of $u_0$. Expanding a temperature fluctuation in real spherical harmonics as $u = \sum a_{lm} Y_{lm}$ and $u_0 = \sum b_{lm} Y_{lm}$, the solution of Eq. (2.2) for the region outside the mask $\mathbf{x} \in \bar{D}$ is given by

$$a_{lm}^{\text{out}}(\lambda) = \frac{\lambda}{l(l+1) + \lambda} b_{lm}, \tag{2.4}$$

where $a_{lm}^{\text{out}}$'s are real expansion coefficients for the solution outside the mask. Equation (2.4) implies a suppression of modes with $l \gg \sqrt{\lambda}$. In the limit of $\lambda \gg 1$,[2] the minimizer of Eq. (2.2) is called the real harmonic inpainting.

The fluctuation $u(\mathbf{x})$ satisfies the following boundary integral equation (see [31] for further detail):

$$\frac{u(\mathbf{x})}{2} + \int_{\partial D} G(\mathbf{x}, \mathbf{y}) q(\mathbf{y}) \sqrt{g} d\mathbf{y} - \int_{\partial D} H(\mathbf{x}, \mathbf{y}) u(\mathbf{y}) \sqrt{g} d\mathbf{y} = 0, \qquad \mathbf{x} \in \partial D, \tag{2.5}$$

where $G$ is the Green's function of Laplacian $\Delta$, and $H$ is the normal derivative of $G$, $H \equiv \partial G / \partial n$. By discretizing the boundary $\partial D$ into $2N$ elements $\Gamma_j$ and approximating $u$ on $\partial D$ by some low-order polynomials, Eq. (2.5) yields

$$[H]\{u\} = [G]\{q\}, \qquad q \equiv \frac{\partial u}{\partial n}, \tag{2.6}$$

where $\{u\}$ and $\{q\}$ are $N$-dimensional vectors consisting of the boundary values of $u_i$ and their normal derivatives $q_i$, and $[H]$ and $[G]$ are $N \times N$-dimensional coefficient matrices, which are obtained from the integration of the fundamental solution $G(\mathbf{x}, \mathbf{y})$ and its normal derivatives $H(\mathbf{x}, \mathbf{y})$. For constant elements

$$u(\mathbf{x}_j) = u^j = \text{Const.}, \qquad q(\mathbf{x}_j) = q^j = \text{Const. on } \Gamma_j, \tag{2.7}$$

the elements of the matrices are

$$H_{ij} = \begin{cases} \tilde{H}_{ij} & i \neq j \\ \tilde{H}_{ij} - \frac{1}{2} & i = j, \end{cases}$$

where

$$\tilde{H}_{ij} \equiv \int_{\Gamma_j} \frac{\partial G}{\partial n}(\mathbf{x}_i, \mathbf{y}_j) \sqrt{g} d\mathbf{y}, \qquad G_{ij} \equiv \int_{\Gamma_j} G(\mathbf{x}_i, \mathbf{y}_j) \sqrt{g} d\mathbf{y}. \tag{2.8}$$

In terms of the normal derivatives $\{q\}$ that are derived from Eq. (2.6), the reconstructed function $u$ within the masked region $D$ is given by

$$u(\mathbf{x}) = -\int_{\partial D} G(\mathbf{x}, \mathbf{y}) q(\mathbf{y}) \sqrt{g} d\mathbf{y} + \int_{\partial D} H(\mathbf{x}, \mathbf{y}) u(\mathbf{y}) \sqrt{g} d\mathbf{y}, \qquad \mathbf{x} \in D. \tag{2.9}$$

## III. ERROR ESTIMATION

### A. Application to azimuthally symmetric masks

In order to check the robustness of the algorithm developed in Sec II, we carry out Monte Carlo simulations of random Gaussian fluctuations on a unit sphere $u_g$. We generate Monte Carlo realizations from a scale-invariant power spectrum ($n = 1$),

$$C_l = \langle |a_{lm}|^2 \rangle \propto \frac{1}{l(l+1)}, \tag{3.1}$$

which describes the large-angle CMB temperature fluctuations in the Einstein-de Sitter universe.

[1] This is a reasonable requirement for Gaussian random fluctuations, as each component of the gradient is also a Gaussian random variable.

[2] This corresponds to the case where the Gaussian noise of the fluctuation $u$–$u_0$ outside the mask is negligible in comparison with the expected absolute values of gradients $|\nabla u|$. For instance, from the signal-to-noise ratio, one can estimate that $\lambda \gtrsim 10^4$ for the WMAP data at $l < 15$.

We first consider azimuthally symmetric masks with constant galactic latitudes, i.e., we mask region below given galactic latitudes $|b| < \theta_0$. For isotropic random fluctuations, modes with $l \gtrsim \pi/\theta_0$ are not affected by the azimuthal cut very much (except for the overall normalization). Therefore, in the following we shall use only multipoles with $l < l_c$, where $l_c = \pi/\theta_0$. From Eq. (2.4), one can see that this choice of cutoff in harmonic space is roughly equivalent to choosing the control parameter $\lambda$, such that $\lambda = (\pi/\theta_0)^2 = l_c^2$. The number of elements on the boundary necessary for numerically solving the integral Eq. (2.5) depends on the size of the mask. For instance, we discretize the boundary of the mask into 80 linear elements for $\theta_0 = 20°$.

To measure the difference between the reconstructed fluctuation $u(\mathbf{x})$ and the original one $u_g(\mathbf{x})$, we use the $L^2$ norm defined as

$$(a[u])^2 \equiv \int_{S^2} (u[\theta, \phi])^2 d\Omega = \sum_{lm} (a_{lm}^{\rm HI})^2, \tag{3.2}$$

where $d\Omega$ is the infinitesimal area element for a surface of unit sphere, and $a_{lm}^{\rm HI}$ is the spherical harmonic coefficients of the reconstructed map. To reduce the sample variance, we generate 1000 realizations, each of which is masked by the azimuthally symmetric mask and is reconstructed by the developed algorithm. We then calculate the mean relative errors defined as

$$\left(\frac{\Delta a}{a}\right)^2 \equiv \left\langle \frac{\int_{S^2} (u_g[\theta, \phi] - u[\theta, \phi])^2 d\Omega}{\int_{S^2} (u_g[\theta, \phi])^2 d\Omega} \right\rangle, \tag{3.3}$$

where $u_g(\mathbf{x})$ and $u(\mathbf{x})$ are the underlying Gaussian fluctuation and the inpainted (reconstructed) fluctuation, respectively. For comparison, we also compute the relative errors for the fluctuations with the ''naive'' ansatz in which $u = 0$ within the masked region, and $u = u_0$ outside the mask.

As one can see in Fig. 1, some of the missing features within the masked region are reconstructed by the inpainting. Improvements are more conspicuous for odd multipoles.

In Table I, we compare the mean relative errors $(\Delta a/a)^2$ at $l = 1$, 2, 3, 4, and 5 for two azimuthally symmetric masks $|b| < 20°$ and 30°. Compared with the naive cases, our developed algorithm based on harmonic inpainting significantly improves reconstruction of odd multipoles. However, for azimuthally symmetric masks, we find that the inpainted even multipoles are identical with those in the naive case.

This can be explained as follows. The Green's function on a unit sphere is given by $G(\mathbf{x}, \mathbf{y}) = -Q_0(\mathbf{x} \cdot \mathbf{y})/2\pi$, where $2Q_0(\mathbf{x} \cdot \mathbf{y}) = \ln[(1 + \mathbf{x} \cdot \mathbf{y})/(1 - \mathbf{x} \cdot \mathbf{y})]$; thus, we have $G(\mathbf{x}, \mathbf{y}) = G(-\mathbf{x}, -\mathbf{y})$. In other words, the Green's function is invariant under the spatial inversion. Therefore, if the boundary of the masked region is invariant under the spatial inversion, the order of the $2N$-dimensional element

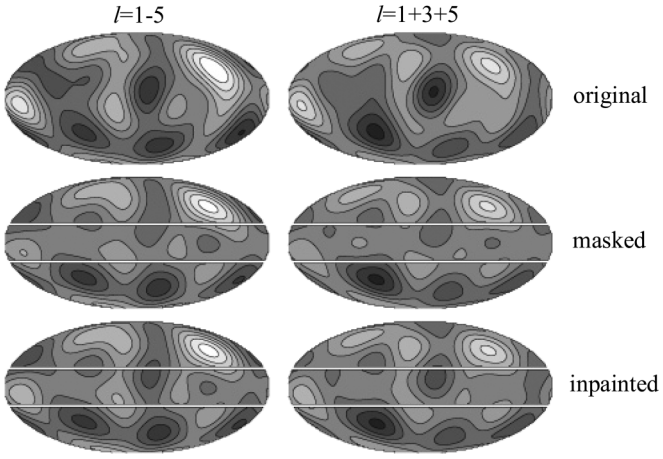


FIG. 1. Contour maps of one Gaussian realization (top), those with an azimuthally symmetric mask $|b| < 20°$ (middle), and the inpainted maps (bottom) in Mollweide projections. The left figures show coadded multipoles (from $l = 1$ to $l = 5$), whereas the right figures show coadded odd multipoles ($l = 1, 3, 5$). The boundaries of the mask are shown in white lines.

TABLE I. Mean relative errors, $(\Delta a/a)^2$, of multipoles for azimuthally symmetric masks with constant galactic latitudes.

| $\lvert b\rvert < 20°$ | | | | | |
|---|---|---|---|---|---|
| $l$ | 1 | 2 | 3 | 4 | 5 |
| naive | 0.23 | 0.21 | 0.55 | 0.39 | 0.55 |
| inpainted | 0.13 | 0.21 | 0.31 | 0.39 | 0.32 |
| $\lvert b\rvert < 30°$ | | | | | |
| $l$ | 1 | 2 | 3 | 4 | 5 |
| naive | 0.39 | 0.37 | 0.76 | 0.58 | 0.62 |
| inpainted | 0.27 | 0.37 | 0.50 | 0.58 | 0.48 |

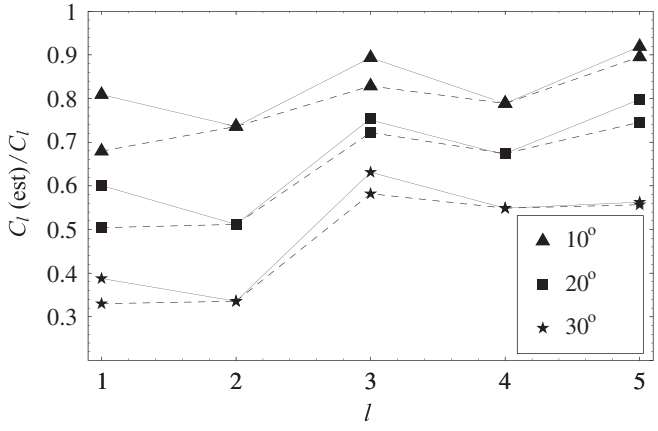


FIG. 2. The estimated (pseudo) power spectrum $C_l(\text{est}) = \sum |a_{lm}|^2/(2l + 1)$ for azimuthally symmetric masks with $|b| < \theta_0 = 10°$, 20°, and 30° divided by the input $C_l \propto (l(l + 1))^{-1}$. The estimated $C_l(\text{est})$ have been averaged over 1000 Monte Carlo realizations, and plotted for the inpainted (reconstructed) fluctuations (solid lines) and for the naive ones (dashed lines).

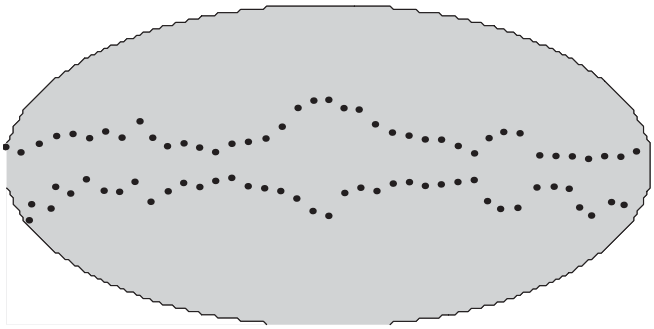

FIG. 3. Meshes on the boundary of the $Kp0$ Galaxy mask, smoothed on scale $\sim$10 arc min.

matrix $[G]$ is reduced to $N$, which kills the degree of freedom for even-parity modes.

The sky cut biases the estimation of the angular power spectrum when it is computed naively as $C_l(\mathrm{est}) = \sum_m (a_{lm}^{\mathrm{HI}})^2/(2l+1)$, which is often called the "pseudo $C_l$" [32]. The effect of mask needs to be deconvolved using, e.g., the Monte Carlo apodised spherical transform estimator method [33]. Here, we do not use the Monte Carlo apodised spherical transform estimator method, but study how much the bias is reduced when we use the naive $C_l$ estimation and the harmonic inpainting. In Fig. 2, we show the ratio of the estimated $C_l$ divided by the input $C_l$, averaged over 1000 Monte Carlo simulations, for three azimuthally symmetric masks, $|b| < 10°$, 20°, and 30°. We find modest improvements at odd multipoles, whereas no improvements are found at even multipoles as they are identical to those in the naive case.

### B. Application to a realistic Galaxy mask

As we have seen, the developed algorithm based on harmonic inpainting fails to reconstruct even multipoles when the Galaxy mask is azimuthally symmetric. However, the shape of the galactic foreground emission region is not perfectly azimuthally symmetric, and thus the corresponding Galaxy mask does not respect parity conservation. Therefore, we expect an improvement for even multipoles as well relative to the naive estimations, once realistic Galaxy masks are used.

To confirm this expectation, we have carried out Monte Carlo simulations with a realistic Galaxy mask. In this study, we also use a realistic sky signal as well: we have generated 1000 realizations of temperature maps from a $\Lambda$CDM model with cosmological parameters given by $(n, \Omega_m, \Omega_\Lambda) = (1, 0.24, 0.76)$. As for the Galaxy mask, we use the WMAP's $Kp0$ mask [21].

Since the shape of the $Kp0$ mask is fairly irregular at the scale of pixels, the definition of the border is not so trivial like the azimuthally symmetric mask in Fig. 1. For instance, some observed pixels close to the mask are surrounded by two or more pixels, some others are completely surrounded by masked pixels, making the choice of the border arbitrary and unstable. To avoid this we have built a smoothed version of the $Kp0$ border. Our procedure consists of going (for a fixed $\phi$ sampled with a constant interval) along the coordinate $\theta$ from Galactic north to

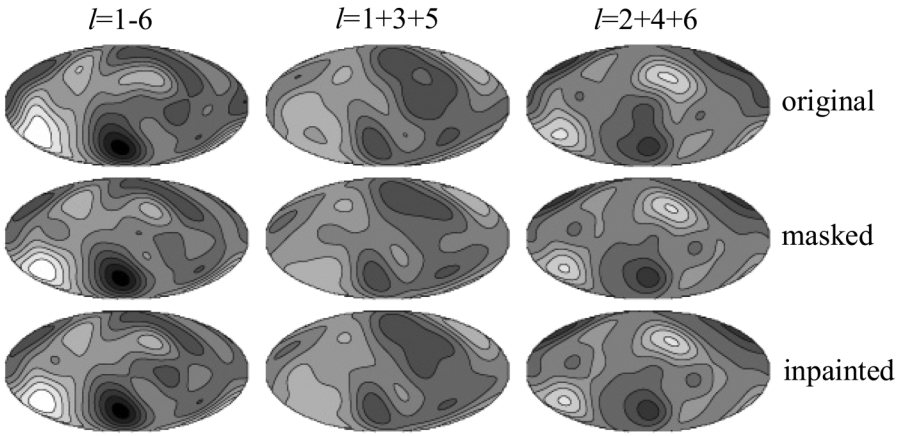


FIG. 4. Contour maps of one Gaussian realization (top), those with a $Kp0$ mask (middle) and the inpainted maps (bottom) in Mollweide projections with galactic coordinates. The left figures show coadded multipoles (from $l = 1$ to $l = 6$), whereas the middle and right figures show coadded odd multipoles ($l = 1, 3, 5$) and coadded even multipoles ($l = 2, 4, 6$), respectively.

TABLE II. Mean relative errors $(\Delta a/a)^2$ of multipoles for the $Kp0$ Galaxy mask.

| $l$ | 1 | 2 | 3 | 4 | 5 | 6 | 7 | 8 | 9 |
|---|---|---|---|---|---|---|---|---|---|
| naive | 0.096 | 0.11 | 0.28 | 0.23 | 0.35 | 0.28 | 0.35 | 0.30 | 0.33 |
| inpainted | 0.053 | 0.10 | 0.15 | 0.21 | 0.21 | 0.27 | 0.24 | 0.29 | 0.25 |

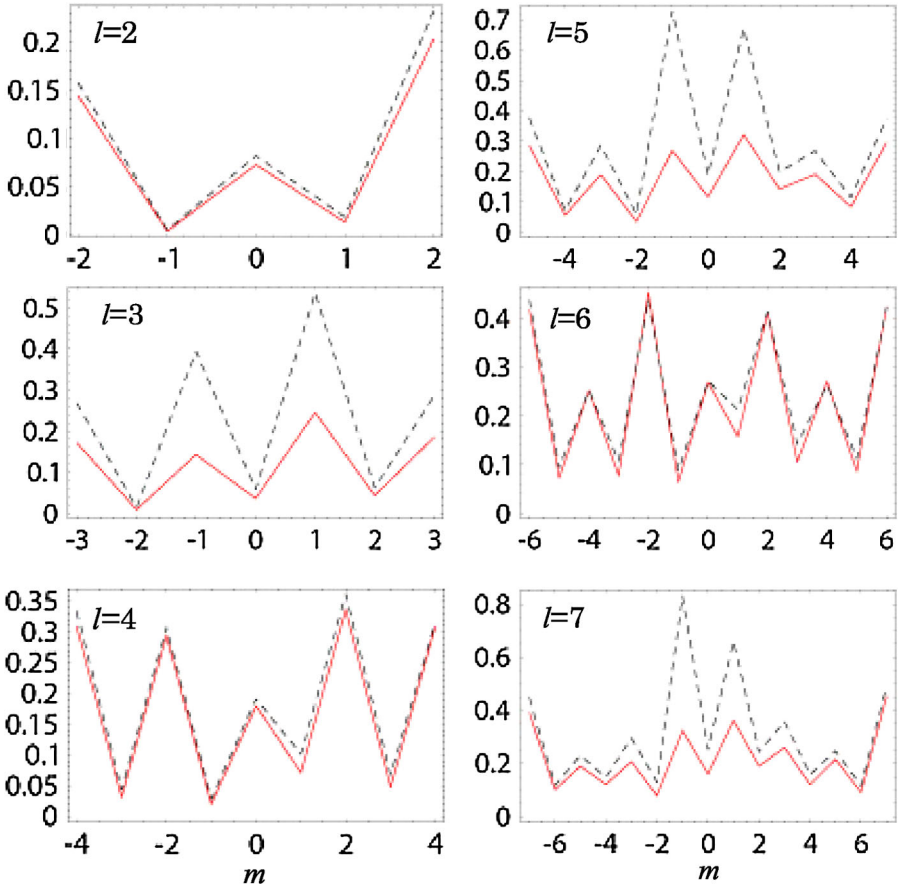


FIG. 5 (color online). Mean relative errors $(\Delta a/a)^2_{(l,m)}$ for the $Kp0$ Galaxy mask. The solid lines and the dashed lines show the inpainted and naive cases, respectively.

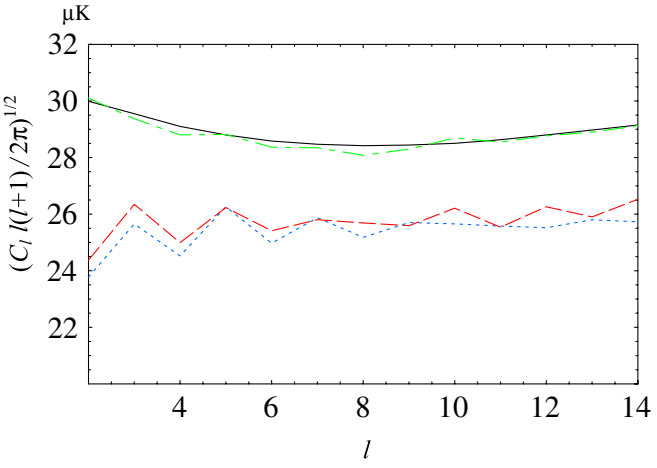


FIG. 6 (color online). The estimated (pseudo) power spectrum $C_l(\text{est}) = \sum |a_{lm}|^2/(2l+1)$ for the $Kp0$ Galaxy mask, averaged over 1000 Monte Carlo realizations. The dashed and dotted lines show $C_l(\text{est})$ from the inpainted map and the map with the $Kp0$ Galaxy mask, respectively. The solid and the dash-dotted lines show the input $C_l$ and the full-sky $C_l(\text{est})$ estimated from 1000 realizations, respectively.

south until we find a masked pixel belonging to the $Kp0$ mask. Once we have found this pixel, we would go back by a step of 10 arcminutes and choose that pixel living on the border. The final set of $(\theta_i, \phi_i)$ defines our border. We found that this procedure regularizes the $Kp0$ border.

We choose the cutoff angular scale to be $l_c = 15$, which corresponds to the mean angular size of the mask in the polar direction. The boundary of the $Kp0$ mask are discretized into 80 linear elements $(\theta_i, \phi_i)$ with a constant interval $2\pi/40$ (Fig. 3).

As in the case of the azimuthally symmetric mask, some of the missing features within the $Kp0$ mask are reconstructed by the inpainting. The improvements are more conspicuous for odd multipoles than even multipoles (Fig. 4).

We show the mean relative errors for the naive estimation and those for the inpainted map with the $Kp0$ mask in Table II. We find that our algorithm improves reconstruction of both the odd and even multipoles, but the improvement for the even multipoles is modest (3 to 10%).

In order to find the polar-angle dependence, we compute the mean relative errors for each $(l, m)$ mode, defined by

$$\left(\frac{\Delta a}{a}\right)^2_{(l,m)} \equiv \left\langle \frac{(a^{\rm HI}_{lm} - a_{lm})^2}{(a^{\rm HI}_{lm})^2} \right\rangle, \tag{3.4}$$

where $a^{\rm HI}_{lm}$ and $a_{lm}$ are real expansion coefficients for the inpainted map and the original map, respectively.

We find that significant improvements come mainly from odd-parity modes with $m = \pm 1$ (Fig. 5). Lower multipoles are improved more by inpainting than higher ones. We also find that the biases in the pseudo $C_l$ are reduced for both the odd and even multipoles (Fig. 6).

## IV. SUMMARY

We have shown that our new algorithm based on harmonic inpainting offers a way to reconstruct the missing CMB temperature anisotropy data within the Galaxy mask, provided that the primordial fluctuation is Gaussian with a scale-invariant ($n = 1$) spectrum. The method reduces the errors for multipoles with an odd parity (odd $l$) significantly. While the method fails to reconstruct multipoles with an even parity (even $l$) for azimuthally symmetric masks, it can reduce the errors for multipoles with an even parity for a more realistic, nonazimuthally symmetric mask, such as the WMAP's $Kp0$ mask. As we have shown, our method is useful for studying the dependence of the CMB at low multipoles given by the azimuthal parameter $m$ of the harmonic coefficients, which is relevant to confirm or confute some of the anomalies at low multipoles found in the WMAP data.

Our new algorithm does not require any specific form of the power spectrum as a prior for reconstructing the missing data as long as the fluctuations obey a Gaussian distribution. Even when fluctuations are not Gaussian, our algorithm is expected to work as long as the fluctuations are sufficiently smooth and the gradients approximately obey a Gaussian distribution. Therefore, our method may be used to reconstruct other observational data that is sufficiently smooth such as radio or infrared maps on a cut sky (a similar technique that can incorporate texture as well as the smooth part is studied in [34]).

Our analysis implies that low multipoles with an even parity are more likely to suffer from the effect of sky cut compared with those with an odd parity. In other words, even-parity modes on large angular scales cannot be precisely reconstructed without assuming specific forms of the angular power. Therefore, the statistical significance of the anomalous features involving the CMB quadrupole may be much lower than claimed, as recent studies suggest [19,20].

The feature of the inpainted 5-yr WMAP data will be explored in the forthcoming paper (Inoue & Cabella 2008).

## ACKNOWLEDGMENTS

Some of the results presented here have been derived using the Healpix package [35]. We acknowledge the use of the Legacy Archive for Microwave Background Data Analysis [36]. Support for LAMBDA is provided by the NASA Office of Space Science. K. T. I. acknowledges the use of computer facility at Yukawa Institute for Theoretical Physics. This work is in part supported by a Grant-in-Aid for Young Scientists (B), Grant No. 20740146 of the MEXT in Japan. E. K. acknowledges support from the Alfred P. Sloan Foundation.

[1] M. Tegmark, A. de Oliveira-Costa, and A. J. S. Hamilton, Phys. Rev. D **68**, 123523 (2003).
[2] A. de Oliveira-Costa, M. Tegmark, M. Zaldarriaga, and A. Hamilton, Phys. Rev. D **69**, 063516 (2004).
[3] P. Vielva, E. Martínez-González, R. B. Barreiro, J. L. Sanz, and L. Cayon, Astrophys. J. **609**, 22 (2004).
[4] M. Cruz, E. Martínez-González, P. Vielva, and L. Cayon, Mon. Not. R. Astron. Soc. **356**, 29 (2005).
[5] H. K. Eriksen, F. K. Hansen, A. J. Banday, K. M. Gorski, and P. B. Lilje, Astrophys. J. **605**, 14 (2004).
[6] F. K. Hansen, A. Balbi, A. J. Banday, and K. M. Gorski, Mon. Not. R. Astron. Soc. **354**, 905 (2004).
[7] L.-Y. Chiang, P. Naselsky, and P. Coles, Astrophys. J. **602**, L1 (2004).
[8] C. J. Copi, D. Huterer, and G. D. Starkman, Phys. Rev. D **70**, 043515 (2004).
[9] C. Park, Mon. Not. R. Astron. Soc. **349**, 313 (2004).
[10] D. J. Schwarz, G. D. Starkman, D. Huterer, and C. J. Copi, Phys. Rev. Lett. **93**, 221301 (2004).
[11] C. Gordon and W. Hue, Phys. Rev. D **70**, 083003 (2004).
[12] T. R. Jaffe, A. J. Banday, H. K. Eriksen, K. M. Gorski, and F. K. Hansen, Astrophys. J. **629**, L1 (2005).
[13] K. Tomita, Phys. Rev. D **71**, 083504 (2005).
[14] K. Tomita, Phys. Rev. D **72**, 043526 (2005); **73**, 029901 (E) (2006).
[15] J. W. Moffat, J. Cosmol. Astropart. Phys. 10 (2005) 012.
[16] L. Campanelli, P. Cea, and L. Tedesco, Phys. Rev. Lett. **97**, 131302 (2006).
[17] K. T. Inoue and J. Silk, Astrophys. J. **648**, 23 (2006).
[18] K. T. Inoue and J. Silk, Astrophys. J. **664**, 650 (2007).
[19] K. Land and J. Magueijo, Mon. Not. R. Astron. Soc. **378**, 153 (2007).
[20] P. D. Naselsky, O. V. Verkhodanov, and M. T. B. Nielsen, arXiv:0707.1484.
[21] C. L. Bennett *et al.*, Astrophys. J. Suppl. Ser. **148**, 97 (2003).

[22] G. Hinshaw *et al.*, Astrophys. J. Suppl. Ser. **170**, 288 (2007).
[23] P. Bielewicz, K. M. Gorski, and A. J. Banday, Mon. Not. R. Astron. Soc. **355**, 1283 (2004).
[24] D. B. Wandelt, D. L. Larson, and A. Lakshminarayanan, Phys. Rev. D **70**, 083511 (2004).
[25] D. L. Larson, H. K. Eriksen, B. D. Wandelt, K. M. Gorski, G. Huey, J. B. Jewell, and I. J. O'Dwyer, Astrophys. J. Suppl. Ser. **656**, 653 (2007).
[26] M. Tegmark, Phys. Rev. D **55**, 5895 (1997).
[27] G. Efstathiou, Mon. Not. R. Astron. Soc. **348**, 885 (2004).
[28] M. Bertalmio, G. Shapiro, V. Caselles, and C. Ballester, in *Proceedings of SIGGRAPH 2000* (ACM Press, New York, 2000), p. 417.
[29] T. Chan and J. Shen, UCLA CAM TR, 00-11, UCLA, 2000.
[30] M. Bertalmio, L. T. Cheng, S. Osher, and G. Shapiro, J. Comput. Phys. **174**, 759 (2001).
[31] K. T. Inoue, PhD thesis, Kyoto University, 2001, arXiv: astro-ph/0103158.
[32] B. D. Wandelt, E. Hivon, and K. M. Górski, Phys. Rev. D **64**, 083003 (2001)
[33] E. Hivon, K. M. Górski, C. B. Netterfield, B. P. Crill, S. Prunet, and F. Hansen, Astrophys. J. **567**, 2 (2002).
[34] P. Abrial, Y. Moudden, J. L. Starck, J. Bobin, M. J. Fadili, B. Afeyan, and M. K. Nguyen, J. Fourier Anal. Appl. **13**, 729 (2007).
[35] K. M. Gorski, E. Hivon, A. J. Banday, B. D. Wandelt, F. K. Hansen, M. Reinecke, and M. Bartelmann, Astrophys. J. **622**, 759 (2005).
[36] Lambda Web site: http://lambda.gsfc.nasa.gov.